# Graphite Nanoplatelet Enabled Embeddable Fiber Sensor for in Situ Curing Monitoring and Structural Health Monitoring of Polymeric Composites

Sida Luo and Tao Liu*

High-Performance Materials Institute, FAMU-FSU College of Engineering, Florida State University, 2525 Pottsdamer Street, Tallahassee, Florida 32310, United States

ABSTRACT: A graphite nanoplatelet (GNP) thin film enabled 1D fiber sensor (GNP-FibSen) was fabricated by a continuous roll-to-roll spray coating process, characterized by scanning electron microscopy and Raman spectroscopy and evaluated by coupled electrical−mechanical tensile testing. The neat GNP-FibSen sensor shows very high gauge sensitivity with a gauge factor of ∼17. By embedding the sensor in fiberglass prepreg laminate parts, the dual functionalities of the GNP-FibSen sensor were demonstrated. In the manufacturing process, the resistance change of the embedded sensor provides valuable local resin curing information. After the manufacturing process, the same sensor is able to map the strain/stress states and detect the failure of the host composite. The superior durability of the embedded GNP-FibSen sensor has been demonstrated through 10 000 cycles of coupled electromechanical tests.

KEYWORDS: graphene, graphite, nanoparticles, composites, sensors, fiber
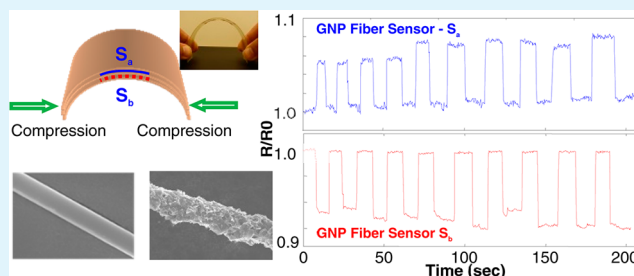
INTRODUCTION

A structure health monitoring (SHM) system is a system-level technology in detection, identification, quantification, and decision about the health states of different high-performance structures, e.g., composite aviation vehicles and civil infra-structures.[1,2] Noninvasive embeddable sensors and sensor arrays are the crucial components in a successful SHM system. In the past decades, a variety of traditional sensors, which include metal-foil-based strain gages, semiconductors or metal oxide thin or thick films,[3,4] piezoelectric sensors,[5,6] optical fiber sensors,[7−10] eddy-current sensors,[11,12] and magnetostrictive sensors,[13] have been explored for this purpose. More recently, a variety of carbon nanomaterials were investigated for their use in developing the light-weight, noninvasive, embeddable, conformable, multifunctional, and scalable piezoresistive sensors for SHM applications. With the carbon nanotube (CNT) as the sensing materials, different types of CNT-enabled piezoresistive sensors, such as CNT yarn,[14,15] CVD grown fuzzy fiber,[16,17] buckypaper,[18−20] and CNT/polymer composites,[21,22] were developed for strain sensing, damage, and failure detection. In addition to CNTs, graphene and graphite nanoplatelets (GNPs) have also been intensively explored as the smart and multifunctional sensors for SHM applica-tions.[23−27] To name a few, Hou et al.[28] and Eswaraiah et al.,[29] respectively, demonstrated using chemically functionalized graphene-filled PDMS (polydimethylsiloxane) and PVDF (polyvinylidene fluoride) nanocomposites as piezoresistive sensors for stress and pressure measurement. A free-standing graphene ribbon was shown to have a gauge factor (GF) of ∼1.9 when being deformed up to ∼3% strain.[30] With a series of

involved processes that included electron beam lithography (EBL), etching, and transfer, Wang et al.[31] fabricated the rippled graphene structures supported on a PDMS substrate, which were demonstrated to be useful for sensing the large deformation with a GF of −2.0. A similar chemical vapor deposition (CVD) followed by transfer technique has been reported by Lee et al. for large-scale fabrication of thin films of graphene or GNPs. The piezoresistivity of such fabricated graphene thin films was reported to have a GF of 6.1.[32] By manipulating the size and packing density of graphene or GNPs and therefore the effect of tunneling resistance, Zhao et al.[33] recently demonstrated the tunable GFs (∼1−300) for the GNP thin films deposited on a mica substrate by RPECVD (remote plasma enhanced chemical vapor deposition). Given the progress being made, however, the form of the current graphene or GNP-enabled piezoresistive sensors, such as nanoribbon and thin film on a bulk substrate, prevents their use as the embeddable and noninvasive multifunctional sensors in SHM application.

In this paper, we report a novel GNP thin film enabled fiber sensor (GNP-FibSen), which takes a continuous 1D fiber form, to overcome this limitation. With an in-house assembled setup, the GNP-FibSen was fabricated by continuously spraying a thin layer of GNPs onto a selected single fiber filament substrate. Through coupled electrical−mechanical tensile tests, the high sensitivity of a standalone GNP-FibSen (GF ∼ 17) has been

demonstrated in this study. Furthermore, with embedding into a fiberglass prepreg laminated structure, the GNP-FibSen showed very interesting and unique dual functionalities. First, during the composite manufacturing process, the embedded GNP-FibSen sensor was able to provide the valuable local resin curing information. This functionality of the GNP-FibSen provides a means for in-line quality assurance of the composite manufacturing process. Second, after the curing process, the same GNP-FibSen is capable of sensing the strain/stress states as well as the failure of the host structure. In this way, the GNP-FibSen renders the host composite with a self-sensing functionality. The superior mechanical robustness of the embedded GNP-FibSen was demonstrated through 10 000 cycles of coupled electromechanical tests, which resulted in a slight change of ~2.6% on the sensor sensitivity. In comparison to the previously developed graphene or GNP sensors,[28−33] the fabrication of GNP-FibSen is simple, scalable, cost-effective, and environmentally benign. Moreover, the continuous and small diameter fiber form of the GNP-FibSen allows it to be used as the embeddable sensors to be easily and noninvasively integrated into the composite structure at desired orientations and locations for multifunctional applications. It is believed that the novel 1D structure, noninvasiveness, robustness, in situ manufacturing monitoring, as well as large-scale manufacturing and facile deployment capabilities make GNP-FibSen a vantage technique for future applications in local damage detection and strain/stress mapping of lightweight composite structures.

■ EXPERIMENTAL METHODS

Fabrication and Characterization of GNP Thin Film Enabled Fiber Sensors (GNP-FibSen). The GNP dispersion was prepared by sonicating a mixture of 300 mg of graphite powder (CAS # 7782-42-5, particle size <45 um, assay content ≥99.99%, Aldrich) and 70 mg of sodium dodecylbenzensulfonate (SDBS, CAS # 25155-30-10, Sigma-Aldrich) in 100 g of deionized water in an ice bath using a Misonix 3000 probe sonicator (20 kHz). The sonicator was operated in a pulse operation mode (on 10 s, off 30 s) with the power set at 45 W for 8 h. AFM (Veeco Instruments, Inc. Multimode) in tapping mode was applied to examine the size of the as-sonicated GNPs (~1 μm in lateral dimension and a few nanometers in thickness).[27] A single filament glass fiber (part # 223, 20 μm in diameter, Fiber Glast Developments Corp.) was used as the substrate for fabricating GNP-FibSen. Figure 1
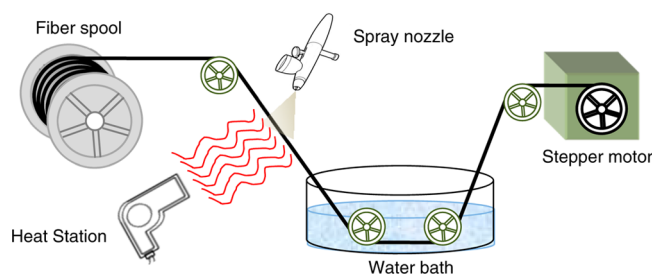

Figure 1. Schematic diagram of the assembly for continuous fabrication of the GNP thin film enabled fiber sensor (GNP-FibSen).

schematically shows the system assembled in-house for implementing a continuous spray coating process in fabricating the GNP-FibSen sensor. In brief, the system was composed of a computer-controlled stepper motor (Silverpak 17C with PW-100-24 power supply, Lin Engineering Corps.) and a series of pulley modules for conveying the fiber filament sequentially through a spray coating station, heating station, and immersion washing station. In a typical coating process, the winding speed was set at ~1 cm/min. The spray coating station was assembled by fixing a spraying nozzle (adjustable nozzle set, part #

AD-NOZ_001, Nanotrons Corp.) on a steel rod to distribute GNP dispersion onto the fiber filament. Downstream of the spray coating station was a heating station used for evaporating water to accelerate the GNP thin film formation. It was composed of a heat gun (Master Heat Gun, HG-301A, 260 °C) set 20 cm distant from the fiber filament. After passing the heating station, the GNP-coated fiber was conveyed through a bath of deionized water to remove the residual SDBS molecules.[34] The washed GNP-FibSen was then dried in air at ambient temperature and ready for later use. The GNP structures of a standalone GNP-FibSen were examined by scanning electron microscopy (SEM) and Raman scattering spectroscopy. SEM was performed with JEOL 7400 at 10 kV for examining the morphologies of the GNP-FibSen sensor. The sample was sputter coated with gold prior to SEM imaging. A Renishaw inVia Raman microscope was used for collecting the Raman spectra of the GNP-FibSen sensor with a 488 nm excitation laser in backscattering geometry.

Fabrication of Glass Fiber Reinforced Composites (GFRC) Embedded with GNP-FibSen. The vacuum bagging process was used to fabricate the fiberglass laminates with Prepreg 7781 E-Glass (part # 3100, 27−33% resin content, 0/90 fiber orientation, Fiber Glass Developments Corp.) to demonstrate the dual functionalities of the embedded GNP-FibSen sensors. In brief, the rectangular shaped prepregs were first stacked into a multilayer structure with the GNP-FibSen sensor(s) and gold wire electrodes (~50 μm diameter, LOT # 29001, California Fine Wire Company) being embedded. The laminate sample prepared for the tension test was composed of a two-layer stack of size 5 cm × 2 cm, and the one for the bending test was composed of a three-layer stack of size 15 cm × 5 cm. Subsequent to the prepreg stacking and sensor embedding, the prepreg stack was then inserted into a vacuum bag to induce the resin curing process. The vacuum bagging process was operated under one standard atmospheric pressure (0.1 MPa) at elevated temperature induced by a hot plate (Manual Hydraulic Press, Specac Corp.) or a vacuum oven. The vendor suggested curing protocols were used; i.e., the temperature was first ramped from room temperature to 143 °C and then maintained at 143 °C isothermally for 2 h. During the curing process, the resistance of the embedded GNP-FibSen was simultaneously recorded by a Keithley 2401 Sourcemeter controlled by a homemade LabVIEW user interface.

Piezoresistivity Evaluation of GNP-FibSen for SHM of GFRC Laminates. A coupled electrical−cyclic tensile test was applied to evaluate the piezoresistivity of the standalone GNP-FibSen sensor at room temperature. In the testing, the fiber sensor, which was glued on perforated cardboard with silver paste applied on the ends as electrodes, was subjected to a cyclic tension deformation applied by a dynamic mechanical analyzer (DMA Q800, TA Instrument Inc.) with the settings of gauge length = 10 mm, displacement amplitude = 0.03 mm, and the displacement rate = 0.3 mm/min. In the meantime, the sensor resistance was recorded by a Keithley 2401 Sourcemeter controlled by a homemade LabVIEW user interface. For a few selected GNP-FibSen sensors (standalone and embedded), the DMA was also used to examine their temperature-dependent resistance behavior by ramping the temperature from 30 to 90 °C at a rate of 5 °C/min. The piezoresistivity of the embedded GNP-FibSen at room temperature was evaluated with an AGS-J mechanical test machine (500 N load cell, Shimadzu Scientific Instruments, Inc.) to apply the cyclic tension to the composite laminate sample. The gauge length of 20 mm and the displacement amplitude of 0.2 mm were used as the settings in AGS-J test. By varying the displacement rate from 1 to 16 mm/min, the loading speed response of the piezoresistivity of the embedded GNP-FibSen was investigated. With the AGS-J settings of gauge length = 20 mm, displacement amplitude = 0.2 mm, and the displacement rate = 2 mm/min, a coupled electrical−mechanical test of 10 000 cycles was applied to a selected laminate sample to test the mechanical robustness of the embedded GNP-FibSen. The same settings were also applied to test the tension to failure response of the embedded GNP-FibSen.

■ RESULTS AND DISCUSSIONS

Structure Characterization and Piezoresistivity Evaluation of the Standalone GNP-FibSen Sensor. As detailed in the Experimental Methods, a scalable roll-to-roll continuous spray-coating process was developed to deposit GNP thin films on a single filament of glass fiber for fabricating GNP-FibSen sensors. Figure 2a shows the optical photograph of a GNP-
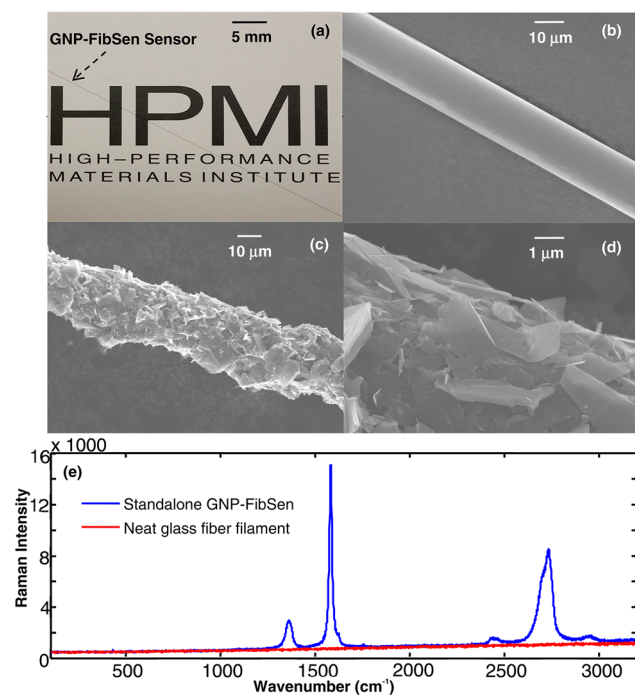

Figure 2. (a) Optical photograph of a standalone GNP-FibSen sensor; (b) SEM image of a neat glass fiber filament, which was used as the substrate for fabricating GNP-FibSen; (c) and (d) SEM images of the GNP packing structures in the GNP-FibSen sensor; and (e) Raman spectra of the standalone GNP-FibSen and the neat glass fiber acquired with a 488 nm laser as the excitation source.

FibSen. The dark visual appearance is an indication of the formation of a dense layer of GNP thin film coated on the glass fiber surface. Further examination of the GNP-FibSen by SEM imaging shows a smooth glass fiber (Figure 2b) coated by an undulated GNP coating (Figure 2c), in which GNP platelets closely packed into a stacked mosaic structure (Figure 2d). The Raman spectrum of the standalone GNP-FibSen is shown in Figure 2e. The signature Raman features[35−37]—D-band at 1361 cm^{-1}, G-band at 1581 cm^{-1}, and the two-component 2D-band around 2730 cm^{-1}—confirm the graphite nanoplatelet structures of the GNP-FibSen that were observed by microscopy techniques (SEM and AFM). The featureless spectrum of a neat glass fiber collected at the same condition was also shown in the same figure for comparison.

With the cyclic tensile strain applied by a dynamic mechanical analyzer (Figure 3a), a coupled electrical−cyclic tensile test was applied to evaluate the piezoresistive response of the standalone GNP-FibSen sensor. The result is shown in Figure 3b. Within the strain range being studied (0−0.3%), the GNP-FibSen sensor shows very good linear piezoresistive response. Namely, the sensor resistance linearly increases with increasing applied tensile strain. One notes the resistance and sensitivity drift of the neat sensor with the number of cyclic tensile tests, which is presumably caused by the sliding/
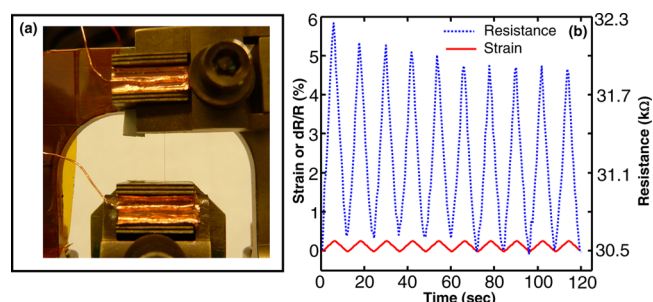

Figure 3. (a) Dynamic mechanical analysis (DMA) setup for testing the piezoresistivity of the standalone GNP-FibSen sensor. (b) The coupled electrical−cyclic tensile test results for the standalone GNP-FibSen fiber sensor. The solid line is the cyclic tensile strain applied by DMA, and the dashed line is the resistance (the right vertical axis) and the resistance change (the left vertical axis) of the sensor.

rearrangement of the graphite nanoplatelets when the sensor is under deformation. As discussed later, the drift issue is improved as the sensor is embedded into a composite structure. According to the definition of the gauge factor (GF) of a piezoresistive sensor

$$GF = \frac{d(\Delta R/R_0)}{d\varepsilon} = \frac{d[(R(\varepsilon) - R_0)/R_0)]}{d\varepsilon} = \frac{1}{R_0}\frac{dR}{d\varepsilon}$$

(1)

where ε is the mechanical strain applied to the sensor; R_0 and R are, respectively, the resistance of the sensor before and after deformation; and the GF of the standalone GNP-FibSen sensor was evaluated to be 17.0 ± 1.3. This value is comparable with that of a GNP thin film sensor deposited on a PET film as reported in our previous work,[27] which is within the range of the graphene and GNP thin films fabricated by different CVD techniques.[31−33]

Embedded GNP-FibSen Sensor for Monitoring the Curing Process of Polymeric Composites. Due to its continuous characteristic and small diameter, the GNP-FibSen sensor can be easily embedded and integrated into the composite structures at desired locations and orientations during the manufacturing process. This is not only beneficial for its use in SHM of the composite structure but also useful as an in situ means for monitoring the polymer resin curing process during the composite manufacturing process. To demonstrate this point, an epoxy/fiberglass laminate sample embedded with a GNP-FibSen sensor was prepared by following a two-stage curing process as described in the Experimental Methods. In the curing process, the sensor resistance was simultaneously recorded. The result is shown in Figure 4a.

As shown in Figure 4a, the sensor resistance rapidly increases from 199.7 to 572.1 kΩ in the first stage of the curing process when the temperature ramps from 25 to 143 °C. The resistance change is as high as ∼186% during this stage. In the subsequent second stage of the curing process, during which the sample was maintained isothermally at 143 °C, the sensor resistance initially manifests a rapid decrease from 572.1 to 466.1 kΩ and then gradually reaches a constant value of 403.6 kΩ. The overall change of the resistance during the second curing stage is ∼−29.5%. The resistance change of the embedded GNP-FibSen during the curing process is not simply a temperature effect but caused by the physical/chemical changes of the resin matrix. To prove this point, the temperature-dependent
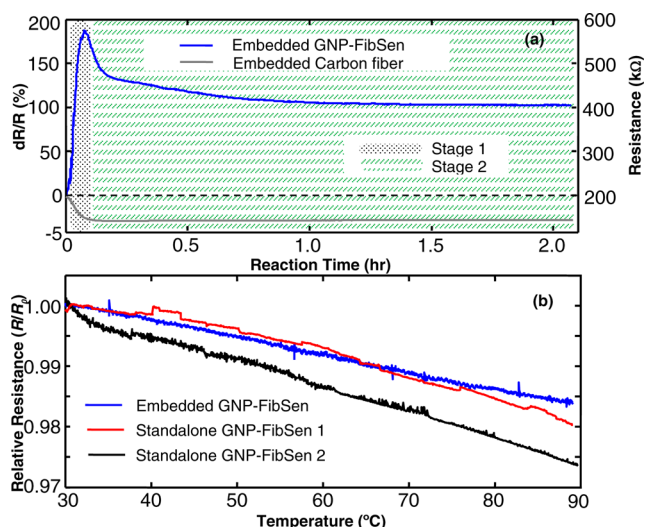
Figure 4. (a) Two-stage curing process induced sensor resistance change for the embedded GNP-FibSen sensor and carbon fiber (CF). Stage 1: temperature ramping from 25 to 143 °C. Stage 2: isothermal at 143 °C for 2 h. (b) Comparison of the temperature-dependent electrical resistance for the standalone GNP-FibSen sensors and the one embedded in a fully cured epoxy/glass fiber composites.

resistance change was tested for the standalone sensor as well as the embedded sensor in the fully cured laminate. Figure 4b shows the results. Clearly, within the temperature range being studied, the resistance change for both the standalone sensors and the sensor embedded in the fully cured laminate all manifest a similar NTC (negative temperature coefficient of resistance) behavior, albeit the coefficient is small. Such NTC behavior is drastically different from the sensor resistance change recorded during the curing process as shown in Figure 4a, where a significant PTC (positive temperature coefficient of resistance) effect occurs in the temperature ramping stage, followed by a resistance decrease in the isothermal stage. The peculiar temperature-dependent resistance change of the embedded GNP-FibSen observed in Figure 4a is attributed to the progressive changes of the viscosity and cross-link density of the epoxy resin matrix during the curing process. In the first stage of the curing process, the resin viscosity decreases with the rapid increase of the temperature from 25 to 143 °C. As a consequence, the resin monomers and oligomers can readily penetrate and infiltrate into the GNP network to cause a large separation and even breakage of GNP–GNP contacts, which therefore induces a significant resistance increase of the GNP-FibSen. In the subsequent isothermal stage of the curing process, the extent of the curing reaction and thus the cross-link density of the resin matrix keep increasing. This induces a significant increase of the resin viscosity and the shrinkage of the resin matrix. As a result, the separation between GNP–GNP contacts is reduced to cause a decrease of the sensor resistance as observed in the beginning of the second stage of the curing process. With further increase of the cross-linking reaction, the system reaches a maximum shrinkage to cause the sensor resistance to stabilize at a constant value. To further corroborate the aforementioned arguments, an epoxy/fiberglass laminate sample embedded with a carbon fiber filament was prepared and tested for its resistance response to the two-stage curing protocols. The rationale for selecting carbon fiber is due to that it has a similar but more densely packed graphitic platelet structure as GNP-FibSen.[38] Unlike the loosely packed

GNP network in GNP-FibSen, the densely packed graphitic structures of the carbon fiber should not be interrupted by the physical/chemical changes of the resin matrix in the curing process. As a consequence, we expect that the resistance change of the carbon fiber in the curing process is simply due to the temperature effect. This is indeed the case as shown in Figure 4a. In the first stage of the curing process, the carbon fiber shows a NTC (negative temperature coefficient of resistance) effect as the temperature ramps from 25 to 143 °C. This NTC behavior is an intrinsic electronic property of carbon fibers.[39,40] As expected, in the second stage of the curing process, the resistance of the carbon fiber maintains a constant since the temperature is isothermally kept at 143 °C. The comparative studies shown in Figure 4 demonstrate the unique capability of the GNP-FibSen in providing valuable information regarding the local physical/chemical changes of the resin matrix during the curing process. Such information cannot be readily accessed by other commonly used techniques, e.g., dynamic mechanical analysis (DMA), differential scanning calorimetry (DSC), infrared spectroscopy (IRS), and optical and dielectric spectroscopy.[41]

Embedded GNP-FibSen Sensor for SHM of the Polymeric Composite Structures. By applying the cyclic tensile strain of 1% in amplitude to the fully cured epoxy/fiberglass laminate (Figure 5a), the piezoresistivity of the embedded GNP-FibSen sensor was evaluated. Figure 5b shows the results of the sensor resistance at different cyclic frequencies (0.04–0.67 Hz). Clearly, the sensor response to the external
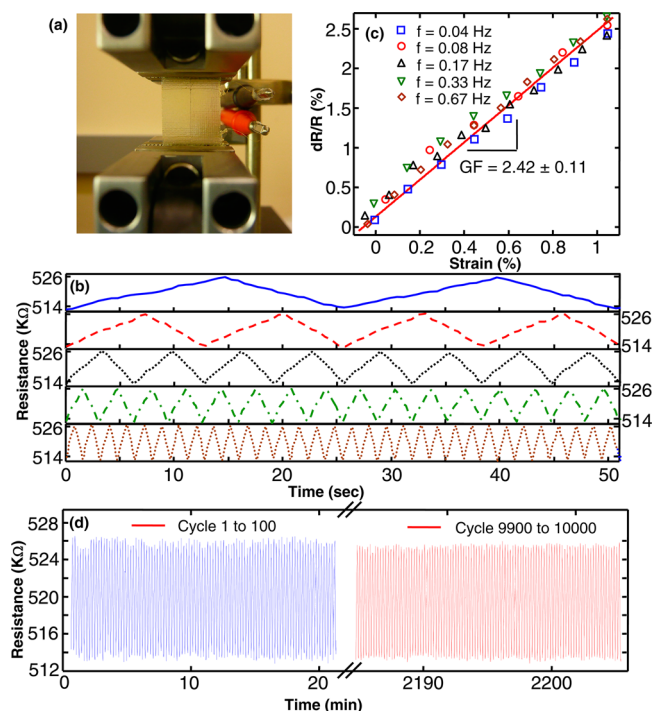

Figure 5. (a) Shimadzu mechanical setup for testing the piezoresistive performance of a GNP-FibSen sensor embedded in fully cured epoxy/glass fiber composites. The piezoresistive response (b) and gauge factor (c) of the embedded fiber sensor under cyclic tensile deformation at various frequencies (from top to bottom: 0.04, 0.08, 0.17, 0.33, 0.67 Hz). (d) Durability test results of the embedded fiber sensor subjected to 10 000 cycles of cyclic tensile test. The blue line is the results for the first 100 cycles, and the red line is for the last 100 cycles.

deformation is instant and shows no frequency dependence. Figure 5c summarizes the GF of the embedded GNP-FibSen sensor tested at different cyclic frequencies. Averaged over the results obtained at different cyclic frequencies, the embedded GNP-FibSen sensor gives a GF = 2.42 ± 0.11. As compared to the standalone sensor (GF = 17.0 ± 1.3), one notes the embedded sensor has a significantly reduced sensitivity. The well-known Poisson effect is believed to be responsible, at least partially, for this phenomenon. As the laminate is under tension in the longitudinal direction of the embedded GNP-FibSen sensor, the transverse direction of the sensor is subjected to compression. The tension causes the sensor resistance increase by increasing the interparticle (GNPs) distance, and the compression induces a decrease of the sensor resistance by decreasing the interparticle (GNPs) distance. These two opposite effects act simultaneously to result in a smaller sensor resistance change and therefore a reduced GF as compared to the standalone GNP-FibSen. Indirect evidence to support this explanation may be found from Hu et al.'s work[42] on the piezoresistivity of the polymer/carbon nanotube composite strain sensor. When the sensor is under tension, the resistance increases, and when the sensor is under compression, the resistance decreases. Certainly, the different nature of the GNP–GNP contacts in the standalone and the embedded sensors may also play a role regarding their significantly different gauge sensitivity. In the standalone sensor, there is a direct GNP–GNP contact, but in the embedded sensor, there is very likely an insulating layer of resin molecules to modulate the GNP–GNP contacts. As a consequence, one may expect the different mechanical as well as electrical response for the standalone and the embedded sensors and therefore their piezoresistive response. Regardless of the detailed mechanism(s) for the reduced gauge sensitivity of the embedded GNP-FibSen sensor, it still has a GF comparable to and even higher than that of CNT yarns,[14] "fuzzy" fibers,[16] and CNT-coated glass fiber.[43,44]

To evaluate the durability of the embedded GNP-FibSen sensor, the epoxy/glass fiber laminate sample was subjected to a coupled electrical–mechanical test with 10 000 cycles of cyclic tensile loading (1% in amplitude at a cyclic frequency of 0.08 Hz). Figure 5d shows the sensor resistance recorded for the first and last 100 cycles. Further calculation indicated that, for the first 100 cycles, the sensor resistance at 0% strain has an average value of 513.5 ± 0.3 kΩ, and the averaged GF is 2.40 ± 0.09; for the last 100 cycles, the sensor resistance at 0% strain has an average value of 513.5 ± 0.2 kΩ, and the averaged GF is 2.34 ± 0.06. The minor changes of the sensor resistance and the GF after 10 000 cyclic tensile tests manifest the excellent durability of the embedded GNP-FibSen sensor, which warrants its future application as a reliable sensing system in SHM of high-performance polymeric composite structures.

An epoxy/fiber glass laminate sample embedded with a GNP-FibSen sensor was subjected to a tension-to-failure test for demonstrating its capability in detecting the failure of the host structure. Figure 6 shows the results. Under small deformation (<1.2%), the laminate behaves elastically, and the sensor resistance correspondingly shows a linear increase. With further increasing the tensile strain above 1.2%, the laminate shows a plastic yield behavior. In coincidence with the yield of the laminate at ~1.2%, there is a rate decrease of the sensor resistance when compared to that in the elastic deformation regime. The failure of the laminate occurs when the strain increases above 2.5%. Correspondingly, one observes a drastic increase of the sensor resistance. The results shown in
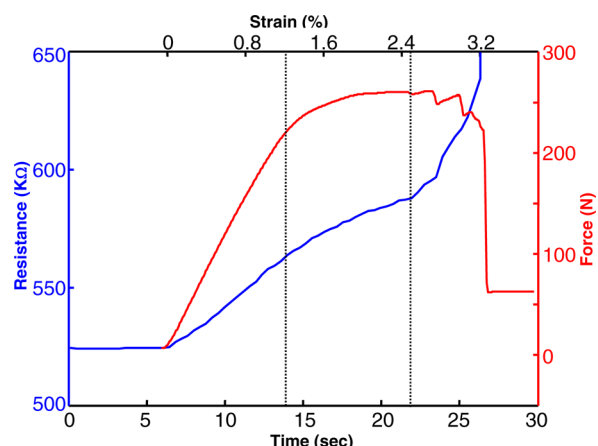

Figure 6. Tension-to-failure test of the fully cured epoxy/fiber glass laminate embedded with a GNP-FibSen sensor. The blue line is the sensor resistance response, and the red line is the force applied to the laminate sample.

Figure 6 suggest the value of the embedded GNP-FibSen sensor in detecting the different failure modes, such as fiber/matrix delamination and crack initiation, of the polymeric composites.

As compared to the previously developed graphene or GNP sensors, the most significant advantage of the GNP-FibSen is that it can be easily and noninvasively integrated into a complex-shaped composite structure at desired orientations and locations for mapping the strain/stress and detecting the local damages. To demonstrate this point, a three-layer epoxy/glass fiber laminate with a curved shape was fabricated and embedded with two GNP-FibSen sensors for sensing different deformation modes. Figure 7a shows the optical graph of the
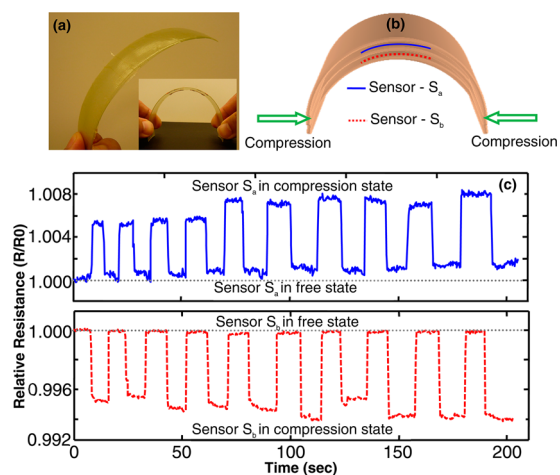

Figure 7. (a) Photo images and (b) schematics of the contour-shaped composite laminates embedded with two GNP-FibSen sensors; S_a and S_b are, respectively, positioned above and below the neutral surface. (c) Resistance response of S_a and S_b when the part is subjected to repeating bending deformation by compressing its two ends manually.

fabricated part. Figure 7b schematically shows the position of the embedded sensors: one (S_a) is positioned above, and the other (S_b) is positioned below the neutral surface. Figure 7c shows the resistance change, respectively, recorded for both S_a and S_b when the part was subjected to repeat bending deformation by compressing its two ends manually. In such a

deformation mode, S_a is under tension, and S_b is under compression. It is noted that, due to the instrumentation limit, the resistances for S_a and S_b were not measured synchronously but separately. This results in the not-in-phase response of S_a and S_b as shown in Figure 7c. Given this limitation, one still can identify that the different deformation modes experienced by S_a and S_b have been nicely captured by their respective resistance changes. That is, while the part was under compression, the resistance of S_a increased, and the resistance of S_b decreased. When the part was in a free state, the resistance of both sensors recovered to their original values.

CONCLUSIONS

With a continuous roll-to-roll spray coating process to deposit graphite nanoplatelets (GNPs) on a glass fiber substrate, the GNP thin film enabled piezoresistive fiber sensors (GNP-FibSen) were developed. The standalone sensor was evaluated by the coupled electrical−mechanical test to show excellent gauge sensitivity. Moreover, the GNP-FibSen sensors were integrated into epoxy/fiber glass composite laminate to demonstrate their utility for life-long structure health monitoring of polymeric composite structure. During the composite manufacturing process, the embedded GNP-FibSen sensor is able to provide the in situ resin curing information. After the manufacturing process, the fiber sensor proves to be useful for mapping the strain and stress states as well as for detecting the failures of the host composite structure. The unique continuous 1D fiber form of the GNP-FibSen sensors allows them to be readily and noninvasively embedded into a complex shaped composite structure at desired orientations and locations. This in conjunction with their multipurpose sensing capabilities make the GNP-FibSen highly valuable for life-long (from manufacturing to failure) structural health monitoring of high-performance polymeric composites. It should be mentioned that, in its current form, the GNP-FibSen sensor is only applicable for nonconducting composite structures. Further development work is needed to insulate the GNP-FibSen such that it can also be applied to conductive composite structures, e.g., carbon fiber reinforced polymeric composites.

AUTHOR INFORMATION

Corresponding Author
*E-mail: liutao@eng.fsu.edu.

Author Contributions
The manuscript was written through contributions of all authors. All authors have given approval to the final version of the manuscript.

Notes
The authors declare no competing financial interest.

ACKNOWLEDGMENTS

ABBREVIATIONS

GNP, Graphite nanoplatelet; GNP-FibSen, Graphite nanoplatelet-Fiber Sensor; SHM, structure health monitoring; CNT, carbon nanotube; GFRC, glass fiber reinforced composites

REFERENCES

(1) Boller, C.; Chang, F.; Fujino, Y. *Encyclopedia of Structural Health Monitoring*, 1st ed.; Wiley: Hoboken, NJ, 2009.
(2) Chang, F. *Structural Health Monitoring 2013 − a Roadmap to Intelligent Structures*, 1st ed.; DEStech Publications: Lancaster, PA, 2013.
(3) Window, A. L.; Holister, G. S. *Strain Gauge Technology*, 2nd ed.; Elsevier Science Publishers Ltd: New York, NY, 1992.
(4) Moletn, L.; Aktepe, B. Review of Fatigue Monitoring of Agile Military Aircraft. *Fatigue Fract. Eng. Mater. Struct.* **2000**, *23*, 767−785.
(5) Kessler, S. S.; Spearing, S. M.; Soutis, C. Damage Detection in Composite Materials using Lamb Wave Methods. *Smart Mater. Struct.* **2002**, *11*, 269−278.
(6) Qing, X.; Beard, S. J.; Kumar, A.; Ooi, T. K.; Chang, F. Built-in Sensor Network for Structural Health Monitoring of Composite Structure. *J. Intell. Mater. Syst. Struct.* **2007**, *18*, 39−49.
(7) Takeda, N. Summary Report of the Structural Health Monitoring Project for Smart Composite Structure Systems. *Adv. Compos. Mater.* **2001**, *10*, 107−118.
(8) Kister, G.; Wang, L.; Ralph, B.; Fernando, G. F. Self-sensing E-glass Fibers. *Opt. Mater.* **2003**, *21*, 713−727.
(9) Lee, B. Review of the Present Status of Optical Fiber Sensors. *Opt. Fiber Technol.* **2003**, *9*, 57−79.
(10) Culshaw, B. Optical Fiber Sensor Technologies: Opportunities and − perhaps − pitfalls. *J. Lightwave Technol.* **2004**, *22*, 39−50.
(11) Placko, D.; Dufour, I. A Focused-field Eddy Current Sensor for Nondestructive Testing. *IEEE Trans. Magn.* **1993**, *29*, 3192−3194.
(12) Sadler, D. J.; Ahn, C. H. On Chip Eddy Current Sensor for Proximity Sensing and Crack Detection. *Sens. Actuator, A* **2001**, *91*, 340−345.
(13) Kannan, E.; Maxfield, B. W.; Balasubramaniam, K. SHM of Pipes using Torsional Waves Generated by In Situ Magnetostrictive Tapes. *Smart Mater. Struct.* **2007**, *16*, 2505−2515.
(14) Zhao, H.; Zhang, Y.; Bradford, P. D.; Zhou, Q.; Jia, Q.; Yuan, F. G.; Zhu, Y. Carbon Nanotube Yarn Strain Sensors. *Nanotechnology* **2010**, *21*, 305502.
(15) Abot, J. L.; Song, Y.; Vatsavaya, M. S.; Medikonda, S.; Kier, Z.; Jayasinghe, C.; Rooy, N.; Shanov, V. N.; Schulz, M. J. Delamination Detection with Carbon Nanotube Thread in Self-sensing Composite Materials. *Compos. Sci. Technol.* **2010**, *70*, 1113−1119.
(16) Garcia, E. J.; Wardle, B. L.; Hart, A. J.; Yamamoto, N. Fabrication and Multifunctional Properties of a Hybrid Laminate with Aligned Carbon Nanotubes Grown In Situ. *Compos. Sci. Technol.* **2008**, *68*, 2034−2041.
(17) Yamamoto, N.; Hart, A. J.; Garcia, E. J.; Wicks, S. S.; Duong, H. M.; Slocum, A. H.; Wardle, B. L. High-yield Growth and Morphology Control of Aligned Carbon Annotates on Ceramic Fibers for Multifunctional Enhancement of Structural Composites. *Carbon* **2009**, *47*, 551−560.
(18) Kang, I.; Schulz, M. J.; Kim, J. H.; Shanov, V.; Shi, D. A Carbon Nanotube Strain Sensor for Structural Health Monitoring. *Smart Mater. Struct.* **2006**, *15*, 737−748.
(19) Loh, K. J.; Kim, J.; Lynch, J. P.; Kam, N. W. S.; Kotov, N. A. Multifunctional Layer-by-layer Carbon Nanotube-polyelectrolyte Thin Films for Strain and Corrosion Sensing. *Smart Mater. Struct.* **2007**, *16*, 429−438.
(20) Rein, M. D.; Breuer, O.; Wagner, H. D. Sensors and Sensitivity: Carbon Nanotube Buckypaper Films as Strain Sensing Devices. *Compos. Sci. Technol.* **2011**, *71*, 373−381.
(21) Thostenson, E. T.; Chou, T. W. Carbon Nanotube Networks: Sensing of Distributed Strain and Damage for Life Prediction and Self Healing. *Adv. Mater.* **2006**, *18*, 2837−2841.
(22) Gao, L.; Thostenson, E. T.; Zhang, Z.; Chou, T. W. Sensing of Damage Mechanisms in Fiber-reinforced Composites under Cyclic Loading using Carbon Nanotubes. *Adv. Funct. Mater.* **2009**, *19*, 123−130.
(23) Yu, T.; Ni, Z.; Du, C.; You, Y.; Wang, Y.; Shen, Z. Raman Mapping Investigation of Graphene on Transparent Flexible Substrate: the Strain Effect. *J. Phys. Chem. C* **2008**, *112*, 12602−12605.

(24) Kim, Y.; Cha, J. Y.; Ham, H.; Huh, H.; So, D.; Kang, I. Preparation of Piezoresistive Nano Smart Hybrid Material based on Graphene. *Curr. Appl. Phys.* **2011**, *11*, S350−S352.

(25) Li, X.; Zhang, R.; Yu, W.; Wang, K.; Wei, J.; Wu, D.; Cao, A.; Li, Z.; Cheng, Y.; Zheng, Q.; Ruoff, R. S.; Zhu, H. Stretchable and Highly Sensitive Graphene-on-polymer Strain Sensors. *Sci. Rep.* **2012**, *2*, 870.

(26) Chen, Z.; Chen, W.; Gao, L.; Liu, B.; Pei, S.; Cheng, H. Three-dimensional Flexible and Conductive Interconnected Graphene Networks Grown by Chemical Vapour Deposition. *Nat. Mater.* **2011**, *10*, 424−428.

(27) Luo, S.; Liu, T. SWCNT/graphite Nanoplatelet Hybrid Thin Films for Self-temperature-compensated, Highly Sensitive, and Extensible Piezoresistive Sensors. *Adv. Mater.* **2013**, *25*, 5650−5657.

(28) Hou, Y.; Wang, D.; Zhang, X.; Zhao, H.; Zha, J.; Dang, Z. Positive Piezoresistive Behavior of Electrically Conductive Alkyl-functionalized Graphene/polydimethylsilicone Nanocomposites. *J. Mater. Chem. C* **2013**, *1*, 515−521.

(29) Eswaraiah, V.; Balasubramaniam, K.; Ramaprabhu, S. Functionalized Graphene Reinforced Thermoplastic Nanocomposites as Strain Sensors in Structural Health Monitoring. *J. Mater. Chem.* **2011**, *21*, 12626−12628.

(30) Huang, M.; Pascal, T. A.; Kim, H.; Goddard, W. A.; Greer, J. R. Electronic-mechanical Coupling in Graphene from In Situ Nano-indentation Experiments and Multiscale Atomistic Simulations. *Nano Lett.* **2011**, *11*, 1241−1246.

(31) Wang, Y.; Yang, R.; Shi, Z.; Zhang, L.; Shi, D.; Wang, E.; Zhang, G. Super-elastic Graphene Ripples for Flexible Strain Sensors. *ACS Nano* **2011**, *5*, 3645−3650.

(32) Lee, Y.; Bae, S.; Jang, H.; Jang, S.; Zhu, S.; Sim, S. H.; Song, Y. I.; Hong, B. H.; Ahn, J. Wafer-scale Synthesis and Transfer of Graphene Films. *Nano Lett.* **2010**, *10*, 490−493.

(33) Zhao, J.; He, C.; Yang, R.; Shi, Z.; Cheng, M.; Yang, W.; Xie, G.; Wang, D.; Shi, D.; Zhang, G. Ultra-sensitive Strain Sensors based on Piezoresistive Nanographene Films. *Appl. Phys. Lett.* **2012**, *101*, 063112.

(34) Luo, S.; Liu, T. Structure-property-processing Relationships of Single-wall Carbon Nanotube Thin Film Piezoresistive Sensors. *Carbon* **2013**, *59*, 315−324.

(35) Ferrari, A. C.; Meyer, J. C.; Scardaci, V.; Casiraghi, C.; Lazzeri, M.; Mauri, F.; Piscanec, S.; Jiang, D.; Novoselov, K. S.; Roth, S.; Geim, A. K. Raman Spectrum of Graphene and Graphene Layers. *Phys. Rev. Lett.* **2006**, *97*, 187401.

(36) Ferrari, A. C. Raman Spectroscopy of Graphene and Graphite: Disorder, Electron-phonon Coupling, Doping and Nonadiabatic Effects. *Solid State Commun.* **2007**, *143*, 47−57.

(37) Ferrari, A. C.; Basko, D. M. Raman Spectroscopy as a Versatile Tool for Studying the Properties of Graphene. *Nat. Nanotechnol.* **2013**, *8*, 235−246.

(38) Harris, P. J. F. New Perspectives on the Structure of Graphitic Carbons. *Crit. Rev. Solid State Mater. Sci.* **2005**, *30*, 235−253.

(39) Nysten, B.; Issi, J.; Barton, R., Jr; Boyington, D. R.; Lavin, J. G. Microstructure and Negative Magnetoresistance in Pitch-derived Carbon Fibers. *J. Phys. D: Appl. Phys.* **1991**, *24*, 714−718.

(40) Donnet, J.; Wang, T. K.; Rebouillat, S.; Peng, J. C. M. 3rd ed; Marcel Dekker: New York, NY, 1998.

(41) Bang, K. G.; Kwon, J. W.; Lee, D. G.; Lee, J. W. Measurement of the Degree of Cure of Glass Fiber-epoxy Composites using Dielectrometry. *J. Mater. Process. Technol.* **2001**, *113*, 209−214.

(42) Hu, N.; Karube, Y.; Arai, M.; Watanabe, T.; Yan, C.; Li, Y. Investigation on Sensitivity of Polymer/Carbon Nanotube Composite Strain Sensor. *Carbon* **2010**, *48*, 680−687.

(43) Zhang, J.; Liu, J.; Zhuang, R.; Mader, E.; Heinrich, G.; Gao, S. Single MWNT-glass Fiber as Strain Sensor and Switch. *Adv. Mater.* **2011**, *23*, 3392−3397.

(44) Luo, S.; Obitayo, W.; Liu, T. SWCNT Thin Film Enabled Fiber Sensors for Life-long Structural Health Monitoring of Polymeric Composites − from Manufacturing, Utilization to Failure. *Carbon* **2014**, DOI: 10.1016/j.carbon.2014.04.083.

9320

dx.doi.org/10.1021/am5017039 | *ACS Appl. Mater. Interfaces* 2014, 6, 9314−9320